ELSEVIER

Volume 28 Numbers 10–11 30 June 2008 ISSN 0278-4343

CONTINENTAL SHELF RESEARCH

Research Papers

(*Continued on outside back cover*)

www.elsevier.com/locate/csr

Continental Shelf Research 28 (2008) 1261–1272

Contents lists available at ScienceDirect

Continental Shelf Research

journal homepage: www.elsevier.com/locate/csr

Physical processes impacting passive particle dispersal in the Upper Florida Keys

Jerome Fiechter [a,*], Brian K. Haus [a], Nelson Melo [b], Christopher N.K. Mooers [a]

[a] Rosenstiel School of Marine and Atmospheric Science, University of Miami, Miami, FL 33149, USA
[b] Atlantic Oceanographic and Meteorological Laboratory, National Oceanic and Atmospheric Administration, Miami, FL 33149, USA

ARTICLE INFO

Article history:
Received 24 November 2007
Received in revised form
22 February 2008
Accepted 22 February 2008
Available online 13 March 2008

Keywords:
Coral reefs
Lagrangian transport
Western boundary current
Ocean circulation model
Velocity profilers
Larval dispersion

ABSTRACT

Physical processes affecting the dispersion of passive particles (e.g., coral larvae, pollutants) in the Upper Florida Keys are investigated through in situ observations (acoustic Doppler current profilers and surface drifters) and numerical ocean circulation modeling (horizontal resolution: 800 m, vertical resolution: 0.1–1 m). During the study period in August 2006 (set to coincide with an annual coral spawning event), Lagrangian trajectories in the vicinity of the reef tract indicate that alongshelf advection was mainly poleward and due to the subtidal flow of the Florida Current, while cross-shelf advection was mainly onshore and due to wind-driven currents. Tidal currents resulted in predominantly alongshelf displacements, but did not contribute significantly to net passive particle transport on a weekly timescale. Typical advection distances were of the order of 10 to 50 km for pelagic durations of 1 week, with significant variability linked to geographical location. In contrast, the direction of transport from the offshore reefs remained essentially constant (i.e., potential dispersion pathways were limited). In addition, Lagrangian trajectories and progressive vector diagrams in the vicinity of the reef tract indicate that alongshelf variations in the cross-shelf velocity gradient associated with the FC are relatively weak on an alongshore scale of ca. 50 km. For August 2006, the highest particle concentrations typically occur inshore of the reef tract, thereby suggesting that onshore transport associated with wind-driven currents contributes significantly to the local retention of passive organisms (and other tracers) in the Upper Florida Keys. Overall, the results illustrate the necessity of conducting targeted in situ observations and numerical model predictions to quantify the physical processes affecting reef-scale advection, especially in an effort to understand local retention and dispersion mechanisms for larval marine organisms.

1. Introduction

With increasing anthropogenic stress on marine populations, especially in nearshore waters, it becomes more urgent to better understand and more efficiently protect living resources in the coastal ocean. Because of the relationship between juvenile and adult populations, characterizing the distribution and abundance of key species (e.g., commercially targeted fishes or reef-building corals) requires knowledge of the larval dispersal rates and recruitment patterns of those organisms (see Cowen et al., 2002 for a review on population connectivity in marine systems). One of the central issues for the connectivity problem is then to quantify the relative importance of alongshore advection and diffusion versus cross-shore advection and diffusion in the coastal boundary layer, as well as possible modulations due to larval behavior (e.g., horizontal and vertical swimming) (Largier, 2003). Characterizing the connectivity patterns between reefs in a specific region would also help address the issues of externally supplied (open) versus self-sustained (closed) populations, recruitment limitation, and population regulation (Armsworth, 2002).

Along the Florida Keys (FK), the motions of mesoscale and submesoscale frontal features associated with the Florida Current (FC) act as mechanisms modulating the cross-shelf exchange of water masses (Shay et al., 1998; Haus et al., 2004), transport of biological material (Lee et al., 1994; Sponaugle et al., 2003), plankton concentration (Lane et al., 2003), and fish larvae abundance (Limouzy-Paris et al., 1997). External (barotropic) and internal (baroclinic) tidal currents, predominantly semi-diurnal in the FK region, are also expected to contribute to local circulation patterns in the vicinity of the Upper FK (UFK) reef tract (Leichter et al., 1996). In addition to tidal and subtidal flows, wind-driven currents also contribute directly to alongshore and

* Corresponding author. Present address: Ocean Sciences Department, University of California, Santa Cruz, CA 95064, USA. Tel.: +1 831 459 3924; fax: +1 831 459 4882.
E-mail addresses: fiechter@ucsc.edu, jfiechter@yahoo.com (J. Fiechter).

0278-4343/$ - see front matter © 2008 Elsevier Ltd. All rights reserved.
doi:10.1016/j.csr.2008.02.018

cross-shore transport, especially for biological organisms concentrated near the ocean surface. The dominant westward wind regime, with a northward component during the summer months, is fairly coherent and homogeneous in the Straits of Florida (SOF) (Peng et al., 1999). Since the orientation of the UFK coastline and reef tract is roughly SW to NE, both Ekman and Stokes drift transports associated with the summer wind conditions will typically have an onshore component.

Previous modeling studies of larval transport in the SOF region have indicated that the interactions between vertical diurnal migration, tidal currents, and salinity gradients may have important effects on the spatial abundance and distribution, as well as the larval dispersal distances, of pink shrimp larvae (Wang et al., 2003; Criales et al., 2005). Larval transport modeling efforts elsewhere have also attempted to predict both short- and long-range larval dispersal/recruitment patterns for diverse marine organisms. For an offshore reef along the Great Barrier Reef, dispersal rates for coral larvae are strongly dependent on reef-scale physical processes (Wolanski et al., 1989), including alongshore currents, tidally driven recirculations, and topographically controlled fronts. In the same region, hydrodynamical models have also been used to investigate the dispersal of reef fish larvae, and to characterize self-recruitment levels and metapopulation connectivity (James et al., 2002; Bode et al., 2006). In particular, the studies illustrate the importance of a few single reefs in maintaining population connectedness and thus allowing transfer of genetic information between subregions of the domain. For Caribbean reef fishes, biophysical modeling studies suggest that the dispersal distances important on ecological time scales are of the order of 10–100 km, and that self-recruitment must be supplemented by outside larval import to sustain most Caribbean fish populations (Cowen et al., 2006).

In the present study, a combination of in situ observations and ocean circulation modeling is used to investigate the complex interactions between the reef tract topography and the FC subtidal, tidal, and local wind-driven currents, as well as their potential impact on Lagrangian transport and larval dispersal pathways in the UFK. Specific interest resides in quantifying alongshelf and cross-shelf transport in relation to larval dispersion following an annual spawning event of *Montastrea faveolata*, one of the major reef-building coral species in the UFK, in August 2006. *M. faveolata* larvae are positively buoyant and located near the surface for 2–3 days after being spawned, then acquire a weak vertical swimming ability and gradually migrate downward during their typical pelagic larval duration (PLD) of ca. 1 week (Szmant and Meadows, 2006). Due to the offshore presence of the FC, larval advection distances along the UFK reef tract could potentially range from hundreds of meters to hundreds of kilometers. The specific reef targeted in the present study, Key Largo Dry Rocks, is located ca. 7 km offshore of the UFK coastline (Fig. 1). Dry Rocks is within the jurisdiction of the Florida Keys National Marine Sanctuary, as well as a designated Sanctuary Preservation Area (SPA). The annual *M. faveolata* spawning event was observed by divers at Dry Rocks on 16 August 2006 at ca. 03:00 UTC.

2. In situ observations

Acquiring high-resolution in situ observations is critical for understanding larval transport mechanisms in a shallow-water environment, and for providing a basis for model-data comparisons in the vicinity of the reef tract. For this purpose, a combination of bottom-mounted acoustic Doppler current profilers (ADPs) and surface drifters is used to characterize the physical environment directly inshore and offshore of Dry Rocks.

2.1. Acoustic Doppler current profilers

Two Sontek 1500 kHz autonomous ADPs were deployed on bottom mounts ca. 1.5 km inshore and offshore of Dry Rocks in water depths of ca. 5 and 7 m, respectively (see Fig. 1). This deployment strategy allowed capturing both reef-scale physical processes and offshore mesoscale variability, as well as identifying the dominant cross-shelf and alongshelf transport mechanisms on each side of the reef tract. In the relatively oligotrophic waters along the UFK, these units have been successfully deployed for up to two months without any adverse effects from biological fouling. The use of high frequency acoustics in shallow water allowed ADP measurements to be made within ca. 1 m of the surface and bottom boundaries. A bin size of 0.25 m was used to maximize vertical resolution and obtain measurements as close as

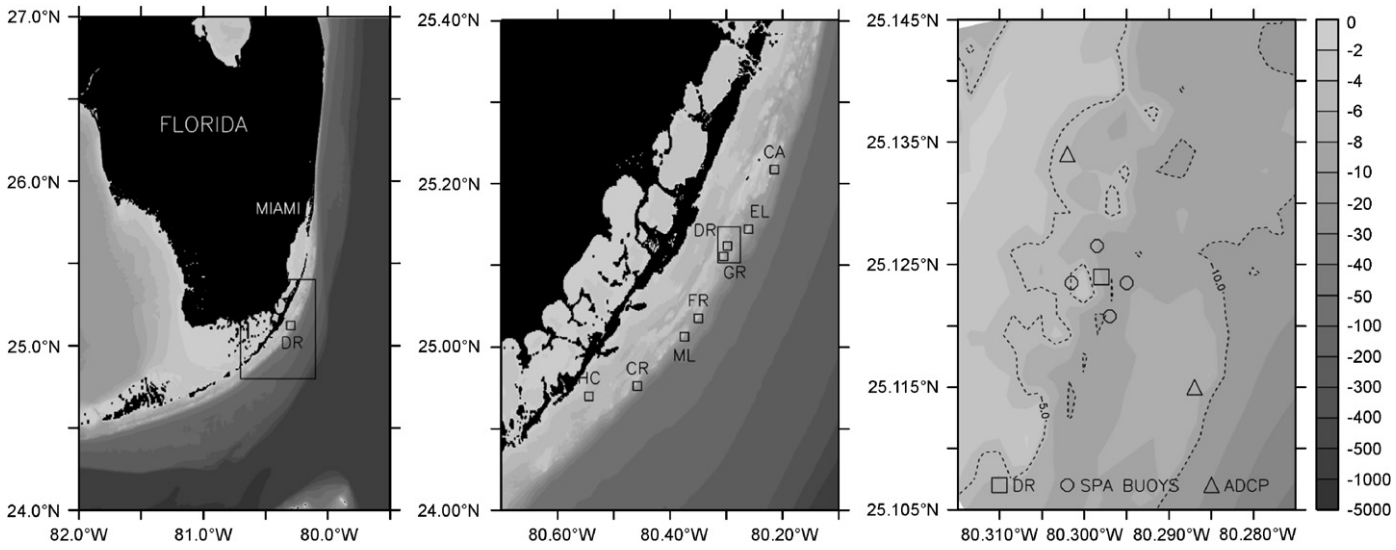

Fig. 1. Geographical map of the Upper Florida Keys reef tract and in situ observations. Left: location of the Upper Florida Keys and Key Largo Dry Rocks (DR). Center: locations of the eight SPA reefs in the Upper Florida Keys (Hen and Chickens (HC), Conch Reef (CR), Molasses Reef (ML), French Reef (FR), Grecian Rocks (GR), Key Largo Dry Rocks (DR), Elbow Reef (EL), and Carysfort Reef (CA)). Right: locations of Key Largo Dry Rocks (DR; square), SPA buoys (circles), and inshore and offshore ADPs (triangles). Gray shades indicate bottom topography (m).

possible to the surface and bottom. This high vertical resolution enables resolving over the shallow shelf the small scale, depth-dependent velocity structure in addition to the barotropic (i.e., depth-independent) flow. Two-minute bursts at a ping rate of 9 Hz were averaged to produce a single velocity profile. The burst sampling was repeated every 10 min over the ca. 60-day measurement period (i.e., from 7 July to 26 August 2006). Due to a hurricane warning in the UFK, the ADP located inshore of Dry Rocks was recovered on 2 August and re-deployed on 11 August at its original location, resulting in a 10-day gap in the velocity record.

2.2. Surface drifters

CODE surface drifters (Davis, 1985) were deployed during the period corresponding to the annual *M. faveolata* spawning event in August. These drifters (drogued in the upper ca. 1 m) were specifically designed to track near-surface currents in coastal waters, with a negligible impact of wave-induced Stokes drift. In addition to the usual ARGOS satellite-tracking system, the drifters were equipped with GPS receivers to increase position accuracy and sampling rate (order of minutes), as required to investigate small-scale circulation in a nearshore reef environment. For the experiment, a cluster of four CODE surface drifters was deployed from Dry Rocks to observe initial advection/dispersion patterns due to near-surface currents. To represent dispersion conditions relative to the whole surface area of the reef, the four drifters were released from each of the SPA buoys (i.e., Marine Sanctuary markers delimiting the Dry Rocks SPA) located ca. 250 m east, west, north, and south of Dry Rocks (see Fig. 1). The three 6-h deployments (on 15, 17, and 22 August 2006) corresponded, respectively, to ca. 12 h before, 36 h after, and 6 days after the *M. faveolata* spawning event observed at Dry Rocks. The 15 August deployment was timed to release the surface drifters ca. 12 h before the predicted spawning time, so the trajectories would correspond to semi-diurnal tidal conditions similar to those expected during the coral spawning event.

3. Ocean circulation and Lagrangian transport models

3.1. Ocean circulation model

The SOF/FK coastal ocean circulation model, called FK-ROMS, is an implementation of the Regional Oceanic Modeling System (ROMS) (Shchepetkin and McWilliams, 2005). The version of ROMS used in the present study is called ROMS-AGRIF, as it includes grid embedding capabilities based on the Adaptive Grid Refinement in Fortran (AGRIF) package (Penven et al., 2006). The grid nesting approach provides the ability to resolve both the regional circulation in the SOF (parent grid) and the local circulation along the FK reef tract (child grid), using only one model configuration (Fig. 2). The one-way nesting (i.e., information is only passed from the parent grid to the child grid) used in FK-ROMS is performed on Cartesian grids, with a 1/32° (ca. 3.2 km) horizontal resolution for the parent grid, and a 1/128° (ca. 800 m) horizontal resolution for the child grid. Both grids have 21 non-uniform sigma levels with refinement in the surface

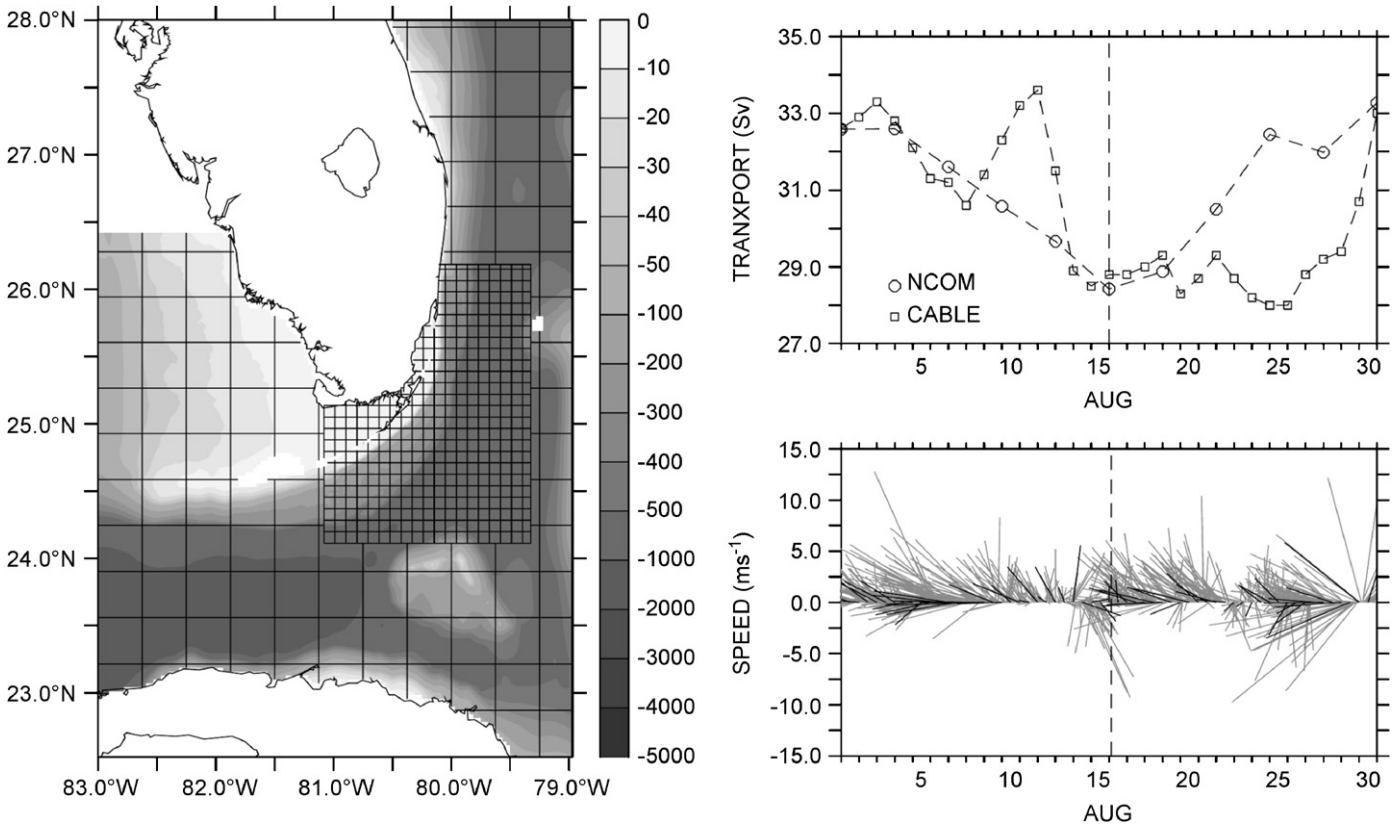

Fig. 2. FK-ROMS model domain and forcing. Left: nested Cartesian parent and child horizontal grid configurations for the Straits of Florida and Upper Florida Keys, with bottom topography (grayscale; m) (grids are subsampled by a factor of 12 for clarity). Upper right: FK-ROMS inflow (western open boundary) transport (S_v; 1 $S_v = 10^6\,m^3\,s^{-1}$) from global NCOM for August, compared with the AOML/NOAA FC cable transport data at 27 N for the same period. Lower right: Comparison between hourly wind observations (gray) from C-MAN station at Molasses Reef (see Fig. 1 for location) and 12-hourly NOGAPS winds (black) interpolated to that location. Vertical dashed lines in upper and lower right panels indicate time of coral spawning event.

layer, which provide a vertical resolution ranging between 0.1 and 100 m depending on the local water depth. The minimum water depth is set to 2 m and extends to the physical location of the coastline.

The bottom topography mapped on the FK-ROMS grids is a blended product between ETOPO 5 (5 min resolution) and the 3-s (ca. 90 m) gridded water depth dataset from the National Geodetic Data Center (NGDC). The resulting bottom topography has therefore sufficient spatial coverage (lacking in the NGDC dataset alone) to include the entire SOF, but yet it provides a very detailed and accurate rendition of the FK reef tract (lacking in the ETOPO 5 dataset alone). However, the 800-m horizontal resolution of the child model is obviously not sufficient to reproduce some of the fine-scale topographic details associated with individual reefs.

FK-ROMS is driven on all open boundaries of the parent grid by synoptic sea surface height, velocity, temperature, and salinity fields from the operational global Navy Coastal Ocean Model (NCOM) (Kara et al., 2006; Mooers et al., 2005), which are updated every third day (Fig. 2). Tidal forcing is derived from the Oregon State University TPXO.6 (Egbert and Erofeeva, 2002) $0.25 \times 0.25^{\circ}$ model for the North Atlantic region and includes eight constituents (M2, S2, N2, K2, K1, O1, P1, and Q1). At the surface, FK-ROMS is forced by a wind stress based on the 12-hourly NOGAPS (Bayler and Lewit, 1992) surface winds (decimated to a $1 \times 1^{\circ}$ application grid) (Fig. 2), and by a net heat flux, shortwave radiation, and surface freshwater flux (E–P) based on the monthly $0.5 \times 0.5^{\circ}$ COADS (Woodruff et al., 1987) climatology. Internal (baroclinic) time steps for the parent and child models are 600 and 200 s, respectively.

3.2. Lagrangian transport model

The Lagrangian particle-tracking model is a simple advection scheme of passive particles based on the local simulated or observed velocities. The model has been used previously to describe sediment transport patterns in a South Florida tidal inlet, and validated to some extent against observed grain-size characteristics (Fiechter et al., 2006). Online and offline trajectory computations indicate that the advection scheme provides adequate accuracy when the temporal resolution of the velocity field is sufficiently high. While the particle-tracking approach does not include a stochastic component, a random-walk or random-flight component (see Griffa, 1996 for a review of Lagrangian stochastic models) could be easily added once the Lagrangian turbulent diffusion parameters near the reef tract are estimated from in situ observations. Furthermore, the high spatial resolution (800 m) of FK-ROMS is arguably sufficient to capture most of the physical processes responsible for the advection and diffusion of the particles and, therefore, minimizes the influence of sub-grid scale processes needing to be represented through the stochastic component.

Since the particle trajectories are based on simulated and observed Eulerian velocity fields, they do not account for the advective component due to the Stokes drift associated with the orbital motion of wind-generated surface gravity waves. A practical approach is to include the effect of Stokes drift on surface trajectories by adding to the Eulerian velocity field an advection velocity in the direction of the wind. Based on existing theoretical evidence (Graber et al., 1997), the magnitude of the Stokes drift is parameterized by using an Eulerian speed equal to 1.5% of the wind speed and an Eulerian direction equal to the wind direction. Since the Stokes drift decays exponentially with depth on the scale of a typical wavelength, its influence on Lagrangian trajectories is significant only for particles located near the surface (i.e., upper ca. 1 m). In the case of the broadcast spawning coral species, the larvae are known to gradually sink during their pelagic duration (Szmant and Meadows, 2006), thus limiting the impact of Stokes drift to the initial (first 72 h) dispersion of the larval patch. The impact of vertical sinking on the transport of coral larvae in the vicinity of the UFK reef tract will be assessed, as a first approximation, by comparing near-surface and near-bottom trajectories.

4. Results

4.1. Model-data comparisons

Since larval dispersion is initially influenced by near-surface currents, FK-ROMS (hourly output) is evaluated against observed (3-h low-passed) currents at 1-m depth. Despite obvious discrepancies, the model predictions reproduce the magnitude of the observed cross-shelf and alongshelf velocity components at

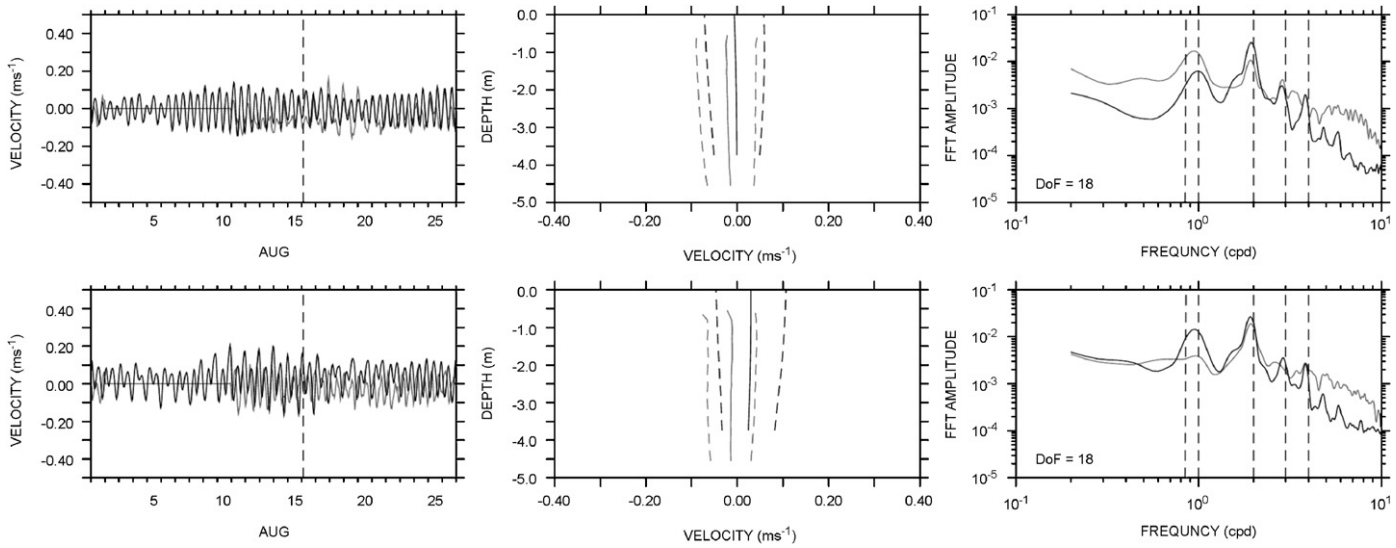

Fig. 3. Inshore comparison between model predictions (black lines) and ADP observations (gray lines) for cross-shelf (upper) and alongshelf (lower) velocity components (positive is NE-ward for alongshelf velocities and SE-ward (offshore) for cross-shelf velocities). Left: velocities ($m\,s^{-1}$) at 1-m depth during August. Center: vertical profiles of August monthly means (solid lines) and standard deviations (dashed lines). Right: spectral (FFT) amplitudes of velocities at 1-m depth for August.

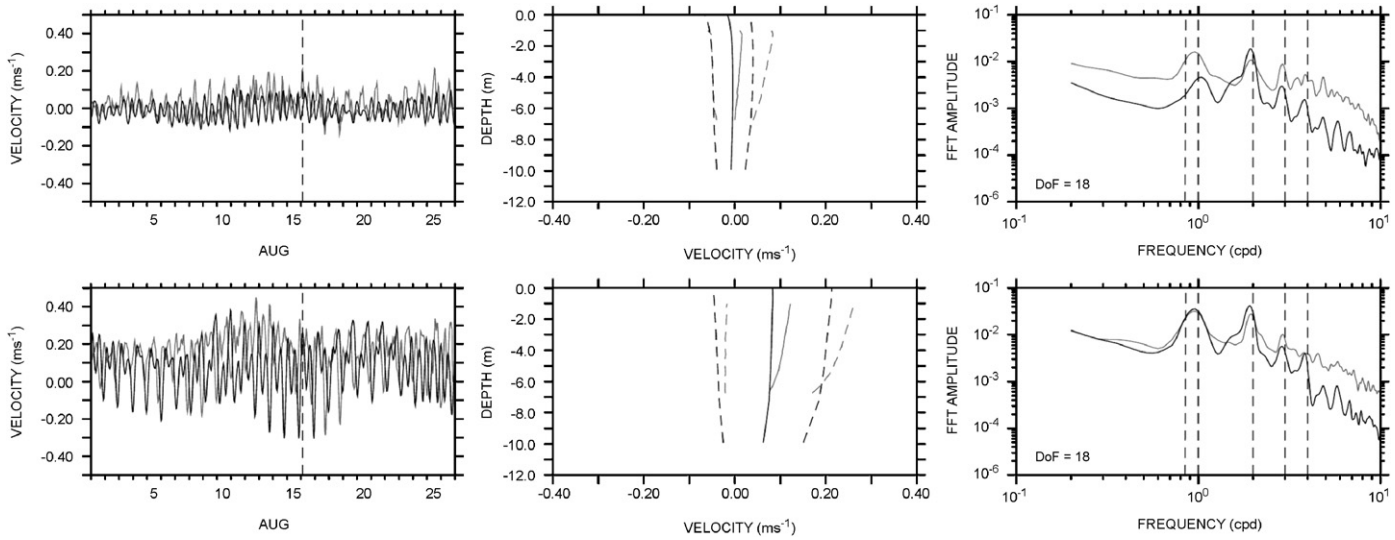

Fig. 4. Offshore comparison between model predictions (black lines) and ADP observations (gray lines) for cross-shelf (upper) and alongshelf (lower) velocity components (positive is NE-ward for alongshelf velocities and SE-ward (offshore) for cross-shelf velocities). Left: velocities (m s^{-1}) at 1-m depth during August. Center: vertical profiles of August monthly means (solid lines) and standard deviations (dashed lines). Right: spectral (FFT) amplitudes of velocities at 1-m depth for August.

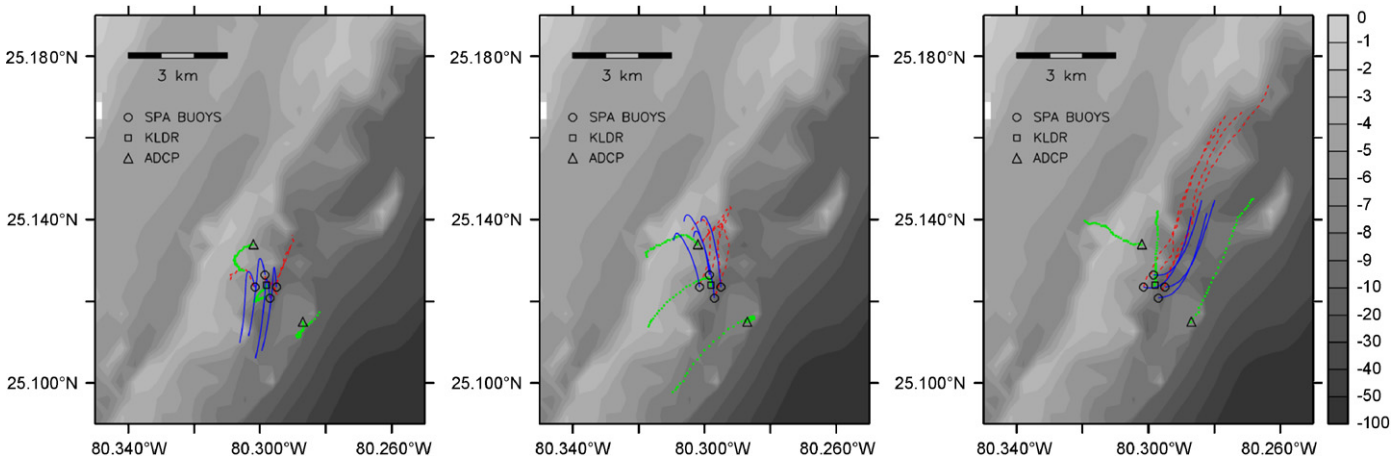

Fig. 5. CODE drifters (red dashed lines), ADP-derived (inshore, offshore, and average) (green dotted lines), and model (blue solid lines) 6-h surface trajectories for deployments starting on 15 August at 14:30 UTC (left), 17 August at 14:00 UTC (center), and 22 August at 13:40 UTC (right). Gray shades indicate bottom topography (m).

1-m depth, as well as some of the variability present in the inshore (Fig. 3) and offshore (Fig. 4) ADP records during August. The differences are mainly attributable to a lack of fine-scale spatial resolution in the bottom topography of FK-ROMS near the reef tract, a lack of temporal resolution in the wind forcing, and, quite possibly, a lack of synopticity in the predicted offshore FC circulation. The agreement between the model and the observations is somewhat better at the inshore location where currents are more tidally dominated. The mean vertical profiles, and associated standard deviations, of predicted cross-shelf and alongshelf velocities confirm that the model reproduces the mean flow conditions and variability inshore of the reef tract. Offshore of the reef tract, the model predictions slightly underestimate the magnitude of the observed mean alongshelf currents, but exhibit a similar range of variability with standard deviations of ca. 0.1 m s^{-1}.

Based on the spectral amplitudes for the cross-shelf and alongshelf velocity components, the model captures most of the variability associated with tidal forcing, and internally generates the 8-hourly shallow-water compound tide (M3) and the dominant M2 6-hourly overtide (M4). Predicted and observed spectra are also in agreement at the semi-diurnal frequency, both inshore and offshore of the reef tract. The diurnal peaks are somewhat less consistent between the model and the observations, with the closest match occurring in the offshore alongshelf velocity spectra. Finally, the model predictions largely reproduce the observed low-frequency (i.e., subinertial) variability, especially for the dominant alongshelf velocity component.

To evaluate the ability to reproduce initial dispersion patterns from Dry Rocks, Lagrangian trajectories based on the model and ADP-measured velocities are compared against observed surface drifter trajectories. The particle trajectories are computed offline with an advection time step of 10 min and using velocities linearly interpolated between hourly model outputs. Particles are released in the model from locations corresponding to those of the drifter deployments (i.e., Dry Rocks SPA buoys). The ADP-derived trajectories (i.e., progressive vector diagrams) are computed based on the 10 min velocities at 1 m depth from the (1) inshore location, (2) offshore location, and (3) average between inshore and offshore locations.

The model trajectories compare favorably with the observed drifter trajectories in predicting the initial dispersion direction for

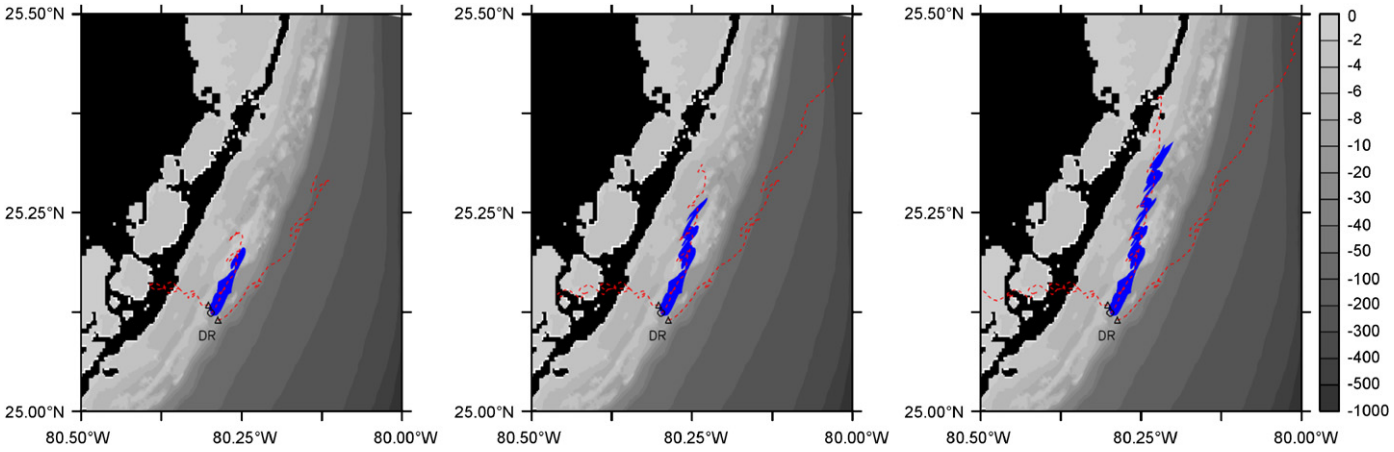

Fig. 6. Model (solid lines) and ADP-derived (inshore, offshore, and average) (dashed lines) surface trajectories for particles released from Key Largo Dry Rocks (DR) during the *Montastrea faveolata* spawning event on 16 August at approximately 03:00 UTC. Left: 3-day trajectories; center: 5-day trajectories; right: 7-day trajectories. Gray shades indicate bottom topography (m).

two of the three deployments (i.e., 17 and 22 August) (Fig. 5). The best agreement is on 17 August, when the initial drifter motion is onshore. On 22 August, the initial poleward motion of the drifters is captured correctly, but the model trajectories underestimate the 6-h dispersion distance by ca. 50%. On 15 August, the near-surface currents in the vicinity of the reef are weak and variable, as indicated by the spread observed in the surface drifter trajectories, and the model trajectories predict less accurately the initial dispersion patterns. With a model resolution of 800 m, this lack of agreement is probably caused by the unresolved small-scale interactions between the flow and the reef topography in weakly forced conditions. As expected, the ADP-derived trajectories at 1-m depth indicate that the agreement with the surface drifter trajectories is closer when using the inshore velocities if the initial motion is onshore (17 August), and the offshore velocities when the initial motion is poleward and alongshelf (22 August). Averaging the velocities between the inshore and offshore ADPs does not seem to improve the prediction for the initial 6 h dispersion observed from the surface drifters during all three deployments.

4.2. Particle trajectories

Based on the level of agreement in the mean and variability of the near-surface currents (vs. the ADP observations), as well as on the ability to predict the initial dispersion patterns in the vicinity of Dry Rocks (vs. the surface drifter trajectories), the model is used to estimate the advection of coral larvae from the reef during the actual spawning event of *M. faveolata* on 16 August 2006 at ca. 03:00 UTC. To evaluate the potential dispersion pattern from the entire surface area of Dry Rocks, 100 particles are released (with a random distribution) within the region defined by the Dry Rocks SPA buoys, and tracked for 7 days (*M. faveolata* PLD is ca. 1 week, as noted above). The model trajectories indicate that advection is mainly alongshelf during the first 3 days, and then more onshore and alongshelf until day 7 (Fig. 6). Despite direction reversals due to tidal current fluctuations, transport is mainly alongshelf and poleward, which is consistent with the mean subtidal velocities near the reef tract. The trajectories based on the ADP velocity observations suggest that larval transport would be mainly onshore at the inshore location, and offshore and poleward at the offshore location. While the averaging approach did not notably improve the prediction for the initial dispersion patterns, the trajectory based on the averaged in situ velocities actually corresponds quite well with the model trajectories in both advection direction and distance. Hence, the velocity averaging method may not work synoptically for tidal currents, but could apply to subtidal currents, which are ultimately responsible for the mean alongshelf transport over multiple tidal cycles (Fig. 7).

To further evaluate the utility of cross-shelf velocity averaging and progressive vector diagrams to predict larval transport in the vicinity of the reef tract, the model is used to emulate in situ observations at the locations of the ADPs inshore and offshore of Dry Rocks (Fig. 8). First, progressive vector diagrams based on (1) predicted velocities at the reef location or (2) predicted velocites averaged between the inshore and offshore locations yield nearly identical trajectories, thereby suggesting that in a physical environment dominated by an alongshelf flow strongly sheared in the cross-shelf direction (e.g., the FC), cross-shelf averaging might provide a reasonable estimation of changes in alongshore velocities across the reef tract. Second, particle trajectories and progressive vector diagrams based on predicted velocities lead to largely similar estimates of larval transport inshore of, at, and offshore of the reef tract, which implies that alongshelf variations in the cross-shelf velocity gradient associated with the FC are relatively weak on an alongshore scale of 50 km. This remark is again presumably valid only for particular synoptic conditions and physical environments, such as the UFK, characterized by a strong alongshelf flow and a fairly uniform daily mean wind field over comparable length scales.

Finally, to isolate the transport component due to wind-driven currents, particle trajectories based on model predictions with and without wind forcing are compared for the week following the *M. faveolata* spawning event. Over the 7-day PLD, the predominantly WNW-ward (onshore) winds, typical of summer conditions in the UFK, lead to a distinct onshore transport component (Fig. 9), which is consistent with earlier observations in the region (Haus et al., 2000). Furthermore, the onshore transport due to wind-driven currents results in larval dispersion distances ca. half of those without wind-driven currents where the particles remain on the outer-shelf and are, thus, more strongly influenced by the offshore FC subtidal currents. The first order approximation for the Stokes drift suggests that the associated transport component could significantly influence dispersion patterns, especially as the larval patch is advected onshore where Eulerian flows are typically weaker (Fig. 9). However, the presence of the reef tract itself will limit (due to wave breaking) the amplitude of onshore-propagating surface gravity waves, and, thus, reduce the influence of Stoke drift on

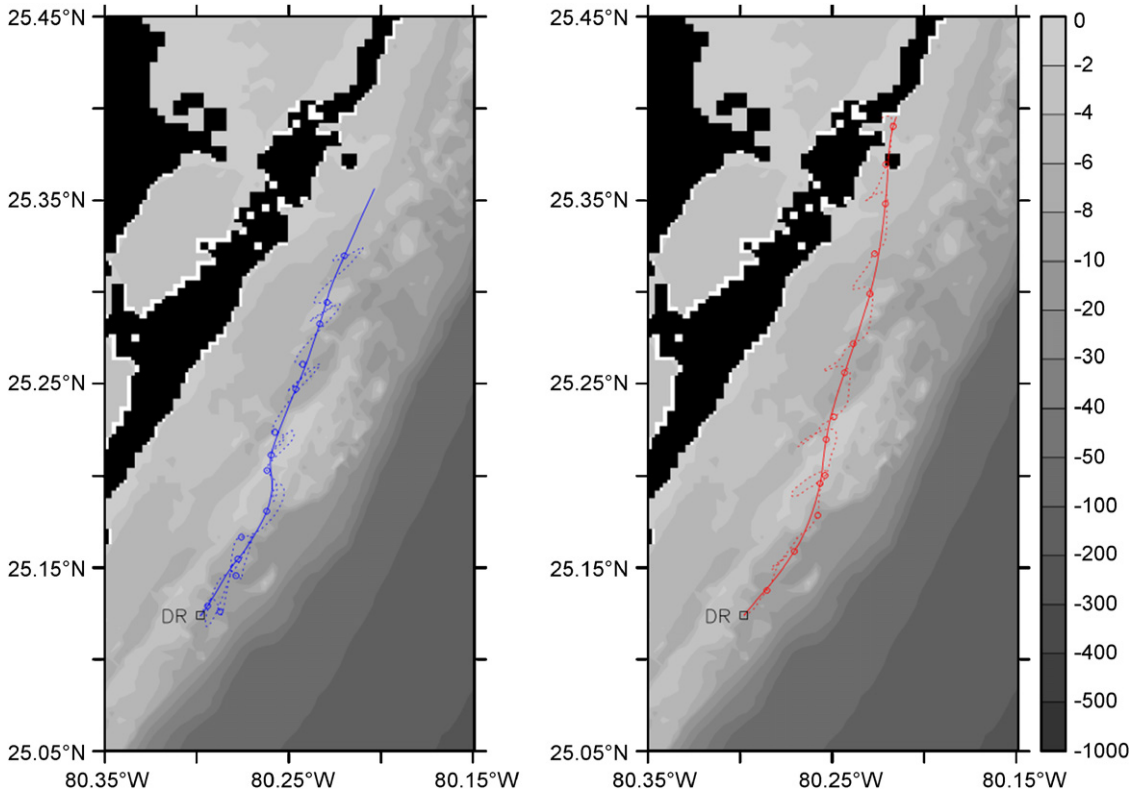

Fig. 7. Model (left) and ADP-derived (average) (right) 7-day surface trajectories using 3-h (dotted line) and 40-h (solid line) low-pass filtered velocities for particles released from Key Largo Dry Rocks (DR) during the *Montastrea faveolata* spawning event on 16 August at approximately 03:00 UTC (symbols indicate 12-hourly positions). Gray shades indicate bottom topography (m).

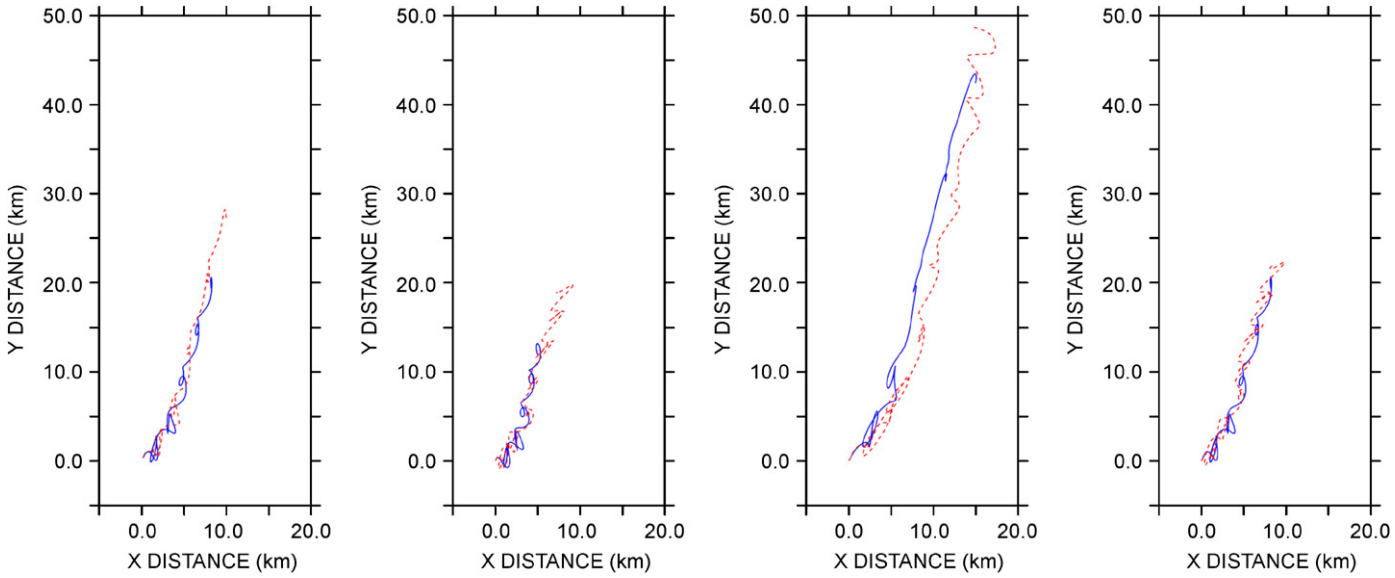

Fig. 8. Particle trajectories and progressive vector diagrams. Far left: 7-day progressive vector diagrams from predicted surface velocities at Key Largo Dry Rocks (solid line) and 7-day predicted surface velocities averaged between inshore and offshore ADP locations (dashed line). Center left: 7-day progressive vector diagram from predicted surface velocities at inshore ADP location (solid line) and 7-day predicted surface trajectory (center of mass) for particles released from inshore ADP location (dashed line). Center right: same as center left, for offshore ADP location. Far right: same as center left, for Key Largo Dry Rocks.

larval transport inshore of the reef tract. Due to the mainly barotropic (depth-uniform) velocity conditions near the reef tract, near-surface and near-bottom trajectories are very similar, except for a slightly more onshore transport near the surface due to the influence of wind-driven currents (Fig. 9). Hence, the gradual sinking of the coral larvae during their PLD is not expected to significantly affect dispersion patterns.

4.3. Dispersal pathways

To provide a statistical description of Lagrangian transport and potential dispersal pathways in the UFK, predicted surface currents for August are used to compute particle trajectories originating from eight major SPA reefs in the UFK (i.e., Hen and Chickens, Conch Reef, Molasses Reef, French Reef, Grecian Rocks,

Dry Rocks, Elbow Reef, and Carysfort Reef) (see Fig. 1). Again, particles are released (with a random distribution) from within the surface areas defined by the SPA buoys delimiting the reefs, so individual trajectories indicate the potential dispersion scatter for coral larvae originating from each location. By releasing 100 particles hourly for 30 days (total of 72,000 particles per reef), the trajectories are representative of the spatial extent over which larval transport might have occurred during August 2006. Probability density functions (PDFs) are computed for each reef for PLDs of 5, 7, and 9 days, and represent spatial particle concentrations based on the native horizontal resolution of the child grid (i.e., particle count in $800 \times 800\,m^2$ grid cells, divided by total number of particles released).

Focusing on the PLD of *M. faveolata*, PDFs at 7 days range between 0.01% and 3.0% for all reefs (Fig. 10). While most of the offshore reefs (i.e., Conch Reef, Molasses Reef, French Reef, Elbow Reef, and Carysfort Reef) indicate concentrations with strong alongshelf shear, Grecian Rocks and Dry Rocks (both located slightly more onshore) exhibit more compact dispersion patterns. Furthermore, larval transport is mainly poleward and onshore for all offshore reef locations, which confirms that subtidal and wind-driven currents are the dominant advective mechanisms on the mid- to outer-shelf. In contrast, larval transport at the inshore location (Hen and Chickens) is mainly alongshelf and evenly distributed on either side of the reef, suggesting that tidal currents are the dominant advective mechanism on the inner-shelf.

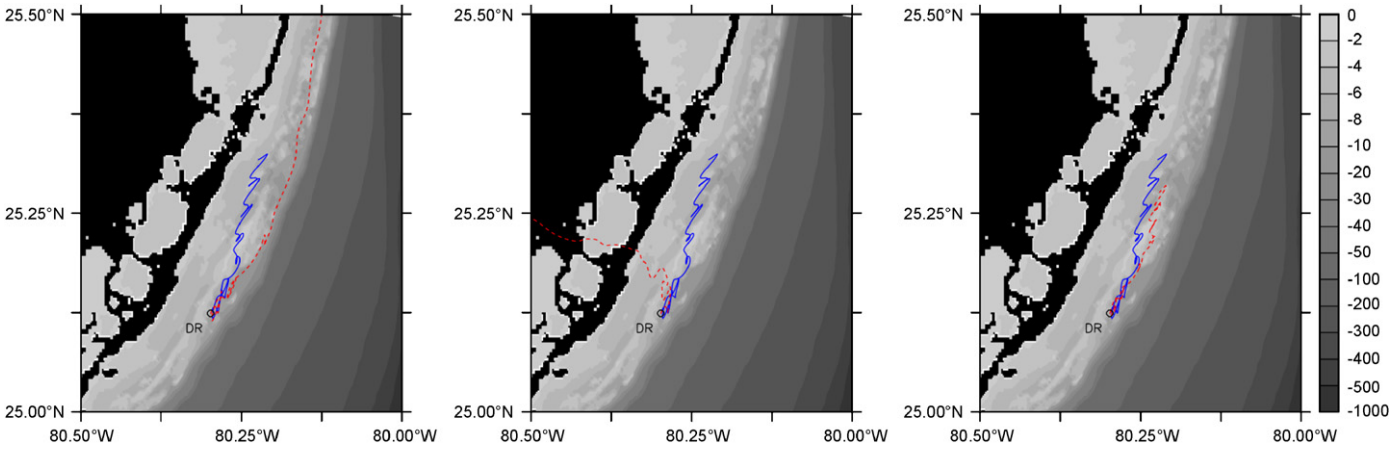

Fig. 9. Influence of surface wind field (left), Stokes drift (center), and vertical migration (right) on 7-day model trajectories for particles released from Key Largo Dry Rocks (DR) during the *Montastrea faveolata* spawning event on 16 August at ca. 03:00 UTC. Left: surface trajectories with (solid line) and without (dahsed line) wind forcing. Center: surface trajectories without (solid line) and with (dashed line) Stokes drift. Right: surface (solid line) and near-bottom (dashed line) trajectories. Gray shades indicate bottom topography (m).

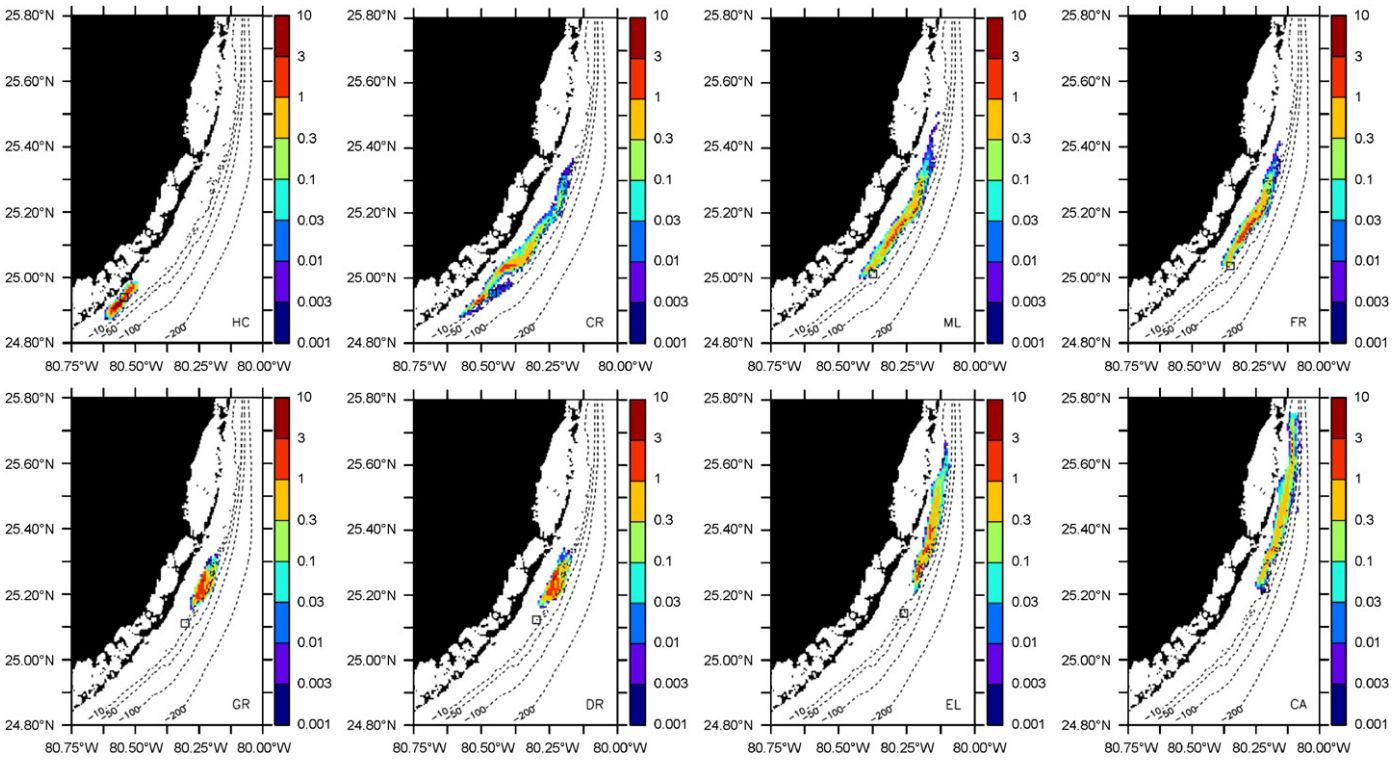

Fig. 10. Predicted probability density functions (%) for pelagic larval duration of 7 days and particles released hourly during August from Hen and Chickens (HC), Conch Reef (CR), Molasses Reef (ML), French Reef (FR), Grecian Rocks (GR), Key Largo Dry Rocks (DR), Elbow Reef (EL), and Carysfort Reef (CA). Contour lines indicate isobaths (m) and square symbol denotes reef locations.

The cumulative PDF for all reefs (i.e., sum of individual PDFs) indicate that for a PLD of 7 days, the highest (ca. 10%) particle concentrations in August 2006 are onshore of the reef tract in the mid- to inner-shelf region (Fig. 11), thereby suggesting that onshore transport due to wind-driven currents is critical for the local retention of passive organisms and particles along the UFK reef tract. Differences between the cumulative PDF after 7 days and those for PLDs of 5 and 9 days further illustrate the wind-driven onshore transport component (with maximum concentrations gradually shifting away from the reef tract and towards the nearshore region), as well as the poleward advection by the subtidal currents associated with the FC circulation.

Since PDFs represent an "averaged" view of particle transport over the entire month of August, changes in contributions from individual releases are useful to identify temporal variability in dispersion pathways from the various reefs. To characterize the contribution of each particle to the cumulative PDF, the two following attributes are examined: (1) radial distance away from the source reef, and (2) direction (i.e., angular position) from the source reef. Again, to relate to *M. faveolata* larval dispersion, the two attributes are computed for a PLD of 7 days (i.e., particle distance and direction from the reef of origin after 7 days of passive transport by surface currents). The hourly model trajectories for August indicate that, while the direction of transport is similar for most offshore reefs and remains essentially constant, transport distances vary significantly with geographical location along the reef tract, as well as temporally from a given reef (Fig. 12). For instance, transport distances can fluctuate between 5 and 30 km at Molassses and French Reefs (southern reefs), and between 10 and 50 km at Elbow and Carysfort Reefs (northern reefs). For reefs located somewhat inshore of the reef tract (i.e., Grecian Rocks and Dry Rocks), transport distances in the range of 10–20 km and exhibit smaller fluctuations. As expected, fluctuations in transport distances are mainly associated with temporal variability of the subtidal currents during August 2006, with periods of enhanced downstream (i.e., poleward) flow resulting in increased transport distances. Furthermore, while tidal currents do not impact significantly the direction of transport from the reef tract, they impose modulations on transport distance from most reefs, with daily variations in the range of 5–10 km depending on geographical location. Interestingly, contributions from tidal currents to the temporal variability in transport distances are

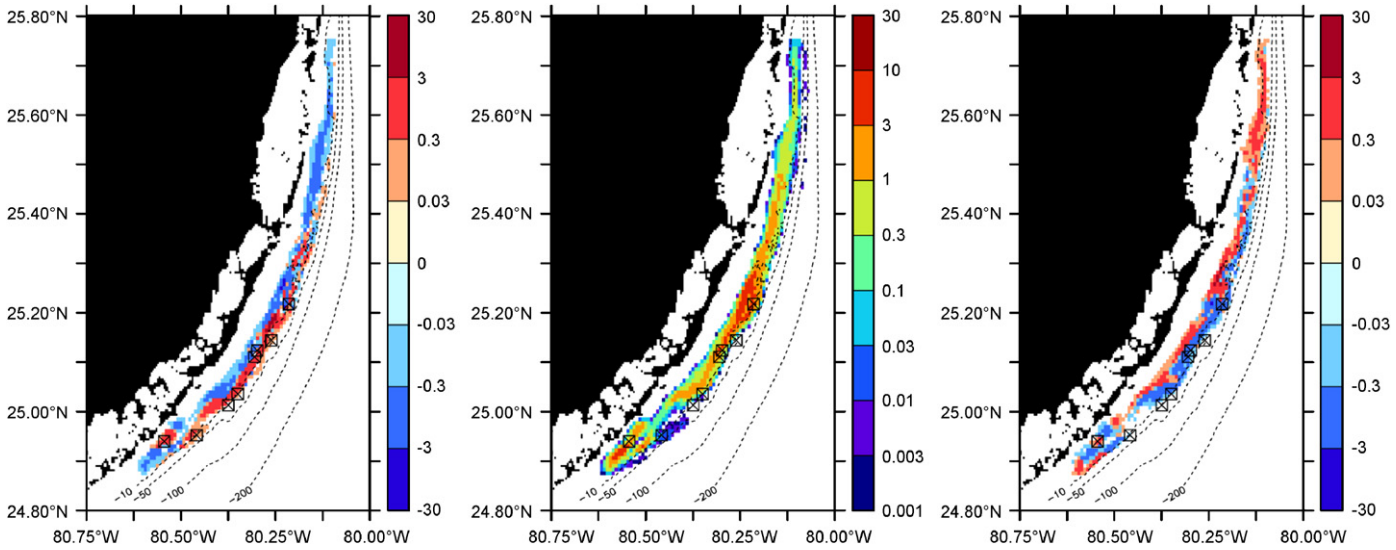

Fig. 11. Predicted cumulative probability density functions (PDF) for particles released hourly during August from all eight reef locations. Left: difference between cumulative PDFs (%) for pelagic larval durations of 5 and 7 days. Center: cumulative PDF (%) for pelagic larval duration of 7 days. Right: difference between cumulative PDFs (%) for pelagic larval durations of 9 and 7 days. Contour lines indicate isobaths (m) and square symbols denotes reef locations.

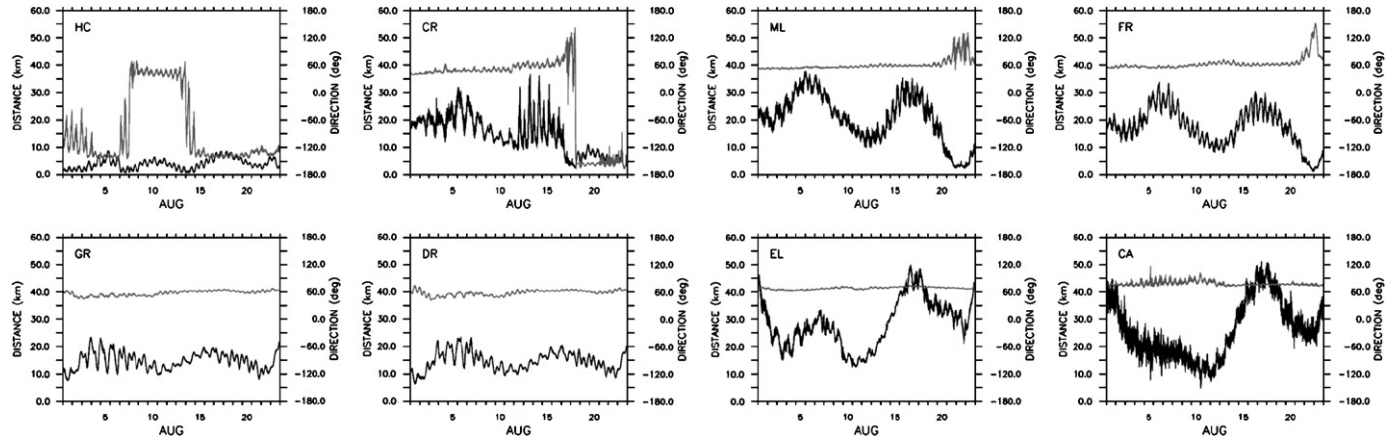

Fig. 12. Distance (black line; km, primary *y*-axis) and direction (gray line; °, secondary *y*-axis) of passive Lagrangian transport after 7 days as a function of particle release time during August 2006 from the reef of origin (Hen and Chickens (HC), Conch Reef (CR), Molasses Reef (ML), French Reef (FR), Grecian Rocks (GR), Key Largo Dry Rocks (DR), Elbow Reef (EL), and Carysfort Reef (CA)). The angle representing the direction of transport is defined on the trigonometric circle (i.e., E = 0°, W = −180/180°, N = 90°, and S = −90°).

largest at Conch Reef, where significant internal tidal activity is known to occur (Leichter et al., 1996).

Finally, the temporal variability in the transport direction for Molasses and French Reefs in late August is presumably related to a rapid shift in wind strength and direction caused by Tropical Storm Chris approaching the UFK. Intriguingly, similar fluctuations in transport direction are not present for the northern reefs (i.e., Grecian Rocks, Dry Rocks, Elbow Reef, and Carysfort Reef), perhaps because of the somewhat larger magnitude of the subtial currents at these locations during that time period.

5. Discussion

5.1. Offshore mesoscale variability

The presence of the FC along the UKF clearly dominates the subtidal circulation offshore of the reef tract and results in a regime where passive particles are rapidly advected downstream (i.e., poleward). However, mesoscale frontal eddies associated with the FC circulation have been linked to enhanced concentrations of larval reef fishes in the region (Sponaugle et al., 2005), suggesting that the flow reversal associated with these cyclonic eddies might have a significant impact on cross-shelf transport. Observational evidence of sub-mesoscale frontal eddy passages along the UFK also indicate an increase in onshore transport during these events, but also suggest that their impact is likely limited to the outer-shelf (i.e., offshore reef tract) and that their net contribution to cross-shelf exchange is smaller than that from the wind-driven currents because of the short residence time and small spatial scales associated with the eddies (Haus et al., 2004). The months of July and August 2006 were particularly quiet in terms of mesoscale eddy activity along the UFK, with only one event detected in the ADP records around 14 July. Progressive vector diagrams based on the observed velocities inshore and offshore of the reef tract during that eddy event suggest an increase in particle retention in the vicinity of the reef tract (Fiechter, 2007). In accordance with the in situ observations, the ocean circulation model did not produce any mesoscale frontal eddy event during August, and, thus, does not provide any insight on the potential influence of FC frontal instabilities on Lagrangian dispersion pathways during the time window corresponding with the coral spawning.

5.2. Wind-driven currents

Because of the two distinct flow regimes inshore (i.e., tidally dominated) and offshore (i.e., FC dominated) of the reef tract, wind-driven currents are expected to have different relative contributions to the subtidal currents as a function of cross-shelf location. As the influence of wind-driven currents on passive particle transport was mainly inferred from the model velocities, comparing the observed currents at 1-m depth from the two ADPs and the observed winds from the C-MAN station at Molasses Reef (not shown) provides an additional element to characterize the potential effects of wind forcing on subtidal currents in the vicinity of the reef tract.

Inshore of the reef tract, subtidal currents are on average 20–60° to the left of the wind vector, but do not respond strongly to changes in the wind direction. While onshore advection during periods of onshore winds is consistent with previous observations in the UFK (Haus et al., 2004), the lack of sensitivity to onshore–offshore shifts in the wind forcing is somewhat surprising. Because the inshore ADP was positioned in only 5 m of water, directly behind the reef tract, and just offshore of a very shallow bank (i.e., 1–2 m deep at the top), the influence of bottom friction and local topography on the observed currents is expected to be large. Furthermore, mean summer winds in the UFK are typically light (i.e., $<5\,m\,s^{-1}$) and, presumably, do not force the inner-shelf circulation as strongly as during winter cold front passages. Offshore of the reef tract, the subtidal flow is clearly dominated by the FC, but wind forcing may contribute to deflecting near-surface currents ca. 10° to the left (i.e., onshore) when the wind direction is typical of summer conditions (i.e., WNW-ward), and ca. 10° to the right (i.e., offshore) when the wind direction is reversed (i.e., SE-ward).

As previous observational studies of surface currents in the UFK have already indicated, the subtidal flow on the shelf is partly related to the wind, but significant variations occur in relation to the local bottom topography (Haus et al., 2000). Hence, the presence of transient Ekman flows with merged bottom and surface boundary layers precludes a simple interpretation of the impact of wind forcing on subtidal currents based on the observed currents at the inshore ADP location. Additional high-resolution (ca. 100 m) numerical simulations and longer (ca. 3–12 months) time series of observed currents in the vicinity of the reef tract would certainly help explore the sensitivity of subtidal currents on the shelf to wind forcing, bottom topography, alongshore atmospheric pressure gradient, FC onshore incursions, and coastally trapped waves.

5.3. Stokes drift

Quantifying the exact contribution of the Eulerian flow to Lagrangian transport in the UFK is further complicated by the fact that the simple parameterization used here for the Stokes drift suggests that its associated transport component may be comparable to those due to subtidal, tidal, and wind-driven currents in the vicinity of the reef tract. However, the presence of the reef tract itself is expected to significantly limit (due to wave breaking) the amplitude of onshore-propagating surface gravity waves, and, as a result, reduce the influence of Stokes drift on particle transport inshore of the reef tract. Furthermore, strong Stokes drifts associated with high wind/wave conditions will also increase the vertical mixing of passive particles, which should in turn reduce overall dispersion distances. To properly address Stokes drift transport, additional investigation is obviously needed to characterize wave–current interactions in the vicinity of an alongshore coastal jet located offshore and reef tract bottom topography.

5.4. Implications for larval transport

For coral larvae, the influence of Stokes drift on larval transport is presumably most significant in the early dispersion stage, when the organisms are positively buoyant and concentrated near the surface. More generally, the gradual sinking of coral larvae during their pelagic duration should not modify considerably their overall dispersion along the UFK, as near-surface and near-bottom trajectories (i.e., the two extremes of vertical migration) result in nearly identical dispersion distances. Certainly more important is the change in transport distance and direction for particle trajectories computed with and without wind forcing applied to the ocean circulation model. The onshore transport component associated with wind-driven currents reduces dispersal distances and acts as a local retention mechanism by transporting passive particles inshore of the reef tract (i.e., inner- to mid-shelf region) on a weekly timescale. This retention mechanism could explain in part the higher percentage of coral coverage and larval recruitment levels observed on nearshore patch reefs compared to

offshore reefs (Chiappone, 1996; Miller et al., 2000). Since pelagic mortality typically reduces larval concentrations by several orders of magnitude, additional physical processes that could locally enhance already existing retention or aggregation regions (e.g., Stokes drift, mesoscale fronts and eddies, vertical mixing) may also have a significant impact on achieving ecologically significant larval concentrations in the region.

To address some of the remaining issues, future studies should be conducted to quantify the importance of turbulent transport (i.e., through introduction of a Lagrangian turbulent eddy coefficient in particle trajectory calculations) for mid- and inner-shelf shallow reef environments, and thus allow a proper parameterization for the addition of a random-walk or a random-flight component to the Lagrangian larval transport model. Furthermore, a simple vertical migratory pattern (e.g., linear sinking over the PLD) could be added to the transport model to identify subregions of the domain where Stokes drift or near-surface wind-driven currents would lead to significant variations in larval transport with depth.

6. Conclusions

While specifically focusing on the larval dispersion of *M. faveolata* after a spawning event in the UFK during August 2006, the combination of targeted in situ observations and numerical ocean circulation modeling revealed fundamental physical processes affecting alongshelf and cross-shelf transport of passive particles in the UFK. In the vicinity of the reef tract, alongshelf advection is mainly poleward and due to subtidal currents associated with the FC, while cross-shelf advection is mainly onshore and due to wind-driven currents. Wind-driven onshore transport also tends to reduce the overall advection distances by keeping larvae inshore of the reef tract where alongshelf velocities are generally weaker. While tidal currents result in predominantly alongshelf displacements, they do not contribute significantly to net transport on a weekly timescale.

For August 2006, the direction of transport from the offshore reefs, mainly dictated by the subtidal FC flow and wind-driven currents, remains essentially constant, thereby suggesting limited potential dispersion pathways in the UFK. In contrast, advection distances for pelagic durations of ca. 1 week vary significantly with location and time of release, ranging from 10 to 50 km for the outer-shelf reefs (i.e., Molasses, French, Elbow, and Carysfort Reefs) and 10 to 20 km for the mid-shelf reefs (i.e., Grecian Rocks and Dry Rocks). While the variability in Lagrangian transport distances is mainly associated with fluctuation in the alongshelf flow of the FC, tidal velocities may locally modulate transport distances (daily variations in the range of 5–10 km depending on geographical location), especially during periods of weaker subtidal currents. Since particle trajectories and progressive vector diagrams based on predicted and observed velocities produce largely similar estimates of larval transport inshore of, at, and offshore of the UFK reef tract, the results suggest that alongshelf variations in the cross-shelf velocity gradient associated with the FC are relatively weak on an alongshore scale of 50 km. Similar conclusions would presumably be valid for other physical environments similarly characterized by a strong alongshelf flow and a fairly uniform daily mean wind field over comparable length scales.

Because of the strong downstream (i.e., poleward) transport associated with the presence of the FC offshore of the reef tract, the wind-driven onshore transport component might be a critical mechanism for the local retention of passive larval organisms in the UFK. However, early settling larvae may be important to maintain self-recruitment and connectivity among the offshore reefs, as maximum larval concentrations gradually shift onshore and away from the reef tract with increasing pelagic duration under the influence of wind-driven currents. In addition to early larval settling, reef-scale turbulent and mixing processes would also play a significant role in retaining larvae near their spawning site and enhancing self-recruitment for the typical PLD associated with *M. faveolata*.

Finally, the present study illustrates the necessity to conduct targeted in situ observations in combination with numerical ocean circulation modeling to characterize the wide range of variability associated with physical processes occurring in a shallow reef environment, and to understand their potential impact on alongshelf and cross-shelf transport of passive particles and other tracers. For larval organisms with a pelagic stage, such studies are a critical component to the identification, and ultimately the protection, of specific source reefs contributing to regional connectivity, while maintaining their own local population through self-recruitment.

Acknowledgments

This research was mainly funded by a grant from the National Oceanic and Atmospheric Administration's Undersea Research Center at the University of North Carolina at Wilmington pursuant to NOAA award number NA03OAR4300088. This research is also a contribution to the Southeast Atlantic Coastal Ocean Observing System (SEACOOS) Program funded by the Office of Naval Research. Dr. Elizabeth Johns, Grant Rawson, and Ryan Smith at NOAA/AOML are thanked for their assistance in planning and conducting the surface drifter deployments. Richard Curry at Biscayne National Park is thanked for his assistance with the ADP deployments. This study was also inspired by discussions with Drs. Alina Szmant at the University of North Carolina at Wilmington, and Christopher Taggart and Barry Ruddick at Dalhousie University. Comments from Dr. James Leichter at the Scripps Institution of Oceanography (UCSD) and one anonymous reviewer are greatly appreciated.

References

Armsworth, P.R., 2002. Recruitment limitation, population regulation, and larval connectivity in reef fish metapopulations. Ecology 83 (4), 1092–1104.

Bayler, G., Lewit, H., 1992. The Navy Operational Global and Regional Atmospheric Prediction System at the Fleet Numerical Oceanography Center. Weather and Forecasting 7 (2), 273–279.

Bode, M., Bode, L., Armsworth, P.R., 2006. Larval dispersal reveals regional sources and sinks in the Great Barrier Reef. Marine Ecology Progress Series 308, 17–25.

Chiappone, M., 1996. Coral Watch Program Summary: A Report on Volunteer and Scientific Efforts to Document the Status of the Reef in the Florida Key National Marine Sanctuary. The Nature Conservancy, Summerland Key, FL, unpublished.

Cowen, R.K., Gawarkiewicz, G., Pineda, J., Thorrold, S., Werner, F., 2002. Population connectivity in marine systems. Report of a Workshop to Develop Science Recommendations for the National Science Foundation, Durango, CO.

Cowen, R.K., Paris, C.B., Srinivasan, A., 2006. Scaling of connectivity in marine populations. Science 311, 522–527.

Criales, M.M., Wang, J., Browder, J.A., Robblee, M.B., 2005. Tidal and seasonal effect of transport of pink shrimp postlarvae. Marine Ecology Progress Series 286, 231–238.

Davis, R.E., 1985. Drifter observations of coastal surface currents during CODE: the method and descriptive view. Journal of Geophysical Research 90, 4741–4755.

Egbert, G., Erofeeva, S., 2002. Efficient inverse modeling of barotropic ocean tides. Journal of Atmospheric and Oceanic Technology 19, 183–204.

Fiechter, J., 2007. Living on the edge of the Florida Current: a study of the physical processes affecting primary production and larval transport. Ph.D. Dissertation, University of Miami, Miami, FL.

Fiechter, J., Steffen, K.L., Mooers, C.N.K., Haus, B.K., 2006. Hydrodynamics and sediment transport in a southeast Florida tidal inlet. Estuarine, Coastal and Shelf Science 70, 297–306.

Graber, H.C., Haus, B.K., Chapman, R.D., Shay, L.K., 1997. HF radar comparisons with moored estimates of current speed and direction: expected differences and implications. Journal of Geophysical Research 102 (C8), 18,749–18,766.

Griffa, A., 1996. Applications of stochastic particle models to oceanographical problems. In: Adler, R., Muller, P., Rozovskii, B. (Eds.), Stochastic Modeling in Physical Oceanography. Birkhäuser, Boston, pp. 114–140.

Haus, B.K., Wang, J.D., Rivera, J., Martinez-Pedraja, J., Smith, N., 2000. Remote radar measurement of shelf currents off Key Largo, Florida, USA. Estuarine, Coastal and Shelf Science 51, 533–569.

Haus, B.K., Wang, J.D., Rivera, J., Martinez-Pedraja, J., Smith, N., 2004. Southeast Florida Shelf circulation and volume exchange: observations of km-scale variability. Estuarine, Coastal and Shelf Science 59 (2), 277–294.

James, M.K., Armsworth, P.R., Mason, L.B., Bode, L., 2002. The structure of reef fish metapopulations: modeling larval dispersal and retention patterns. Proceedings of the Royal Society of London B 269, 2079–2086.

Kara, A.B., Barron, C.N., Martin, P.J., Smedstad, L.F., Rhodes, R.C., 2006. Validation of interannual simulations from the 1/8° global Navy Coastal Ocean Model (NCOM). Ocean Modeling 11, 376–398.

Lane, V.Z., Smith, S.L., Graber, H.C., Hitchcock, G.L., 2003. Mesoscale circulation and the surface distribution of copepods near the south Florida Keys. Bulletin of Marine Science 72 (1), 1–18.

Largier, J.L., 2003. Considerations in estimating larval dispersal distances from oceanographic data. Ecological Applications 13 (Suppl. 1), 71–89.

Lee, T.N., Clarke, M.E., Williams, E., Szmant, A.F., Berger, T., 1994. Evolution of the Tortugas gyre and its influence on recruitment in the Florida Keys. Bulletin of Marine Science 54 (3), 621–646.

Leichter, J.J., Wing, S.R., Miller, S.L., Denny, M.W., 1996. Pulsed delivery of subthermocline water to Conch Reef (Florida Keys) by internal tidal bores. Limnology and Oceanography 41 (7), 1490–1501.

Miller, M.W., Weil, E., Szmant, A.M., 2000. Coral recruitment and juvenile mortality as structuring factors for reef benthic communities in Biscayne National Park, USA. Coral Reefs 19, 115–123.

Mooers, C.N.K., Meinen, C.S., Baringer, M.O., Bang, I., Rhodes, R., Barron, C.N., Bub, F., 2005. Cross validating ocean prediction and monitoring systems. EOS 86 (29).

Limouzy-Paris, C.B., Graber, H.C., Jones, D.L., Roepke, A.W., Richards, W.J., 1997. Translocation of larval coral reef fishes via sub-mesoscale spin-off eddies from the Florida Current. Bulletin of Marine Science 60, 966–983.

Peng, G., Mooers, C.N.K., Graber, H.C., 1999. Coastal winds in South Florida. Journal of Applied Meteorology 38, 1740–1757.

Penven, P., Debreu, L., Marchesiello, P., McWilliams, J.C., 2006. Evaluation and application of the ROMS 1-way embedding procedure to the central California upwelling system. Ocean Modelling 12, 157–187.

Shay, L.K., Lee, T.N., Williams, E.J., Graber, H.C., Rooth, C.G.H., 1998. Effects of low-frequency current variability on near-inertial submesoscale vortices. Journal of Geophysical Research 103 (C9), 18,691–18,714.

Shchepetkin, A.F., McWilliams, J.C., 2005. The regional oceanic modeling system (ROMS): a split-explicit, free-surface, topography-following-coordinate oceanic model. Ocean Modelling 9, 347–404.

Sponaugle, S., Fortuna, J., Grorud, K., Lee, T., 2003. Dynamic of larval fish assemblages over a shallow coral reef in the Florida Keys. Marine Biology 143, 175–189.

Sponaugle, S., Lee, T., Kourafalou, V., Pinkard, D., 2005. Florida Current frontal eddies and the settlement of coral reef fishes. Limnology and Oceanography 50 (4), 1033–1048.

Szmant, A.M., Meadows, M.G., 2006. Developmental changes in coral larval buoyancy and vertical swimming behavior: implications for dispersal and connectivity. In: Proceedings of the 10th International Coral Reef Symposium, Okinawa, pp. 431–437.

Wang, J.D., Luo, J., Ault, J.S., 2003. Flows, salinity, and some implications for larval transport in South Biscayne Bay, Florida. Bulletin of Marine Science 72 (3), 695–723.

Wolanski, E., Burrage, D., King, B., 1989. Trapping and dispersion of coral eggs around Bowden Reef, Great Barrier Reef, following mass coral spawning. Continental Shelf Research 9 (5), 479–496.

Woodruff, S.D., Slutz, R.J., Jenne, R.L., Steurer, P.M., 1987. A comprehensive ocean–atmosphere data set. Bulletin of American Meteorological Society 68, 1239–1250.